



# Biotic and Abiotic Stresses Activate Different $\text{Ca}^{2+}$ Permeable Channels in *Arabidopsis*

Xiao-Qiang Cao<sup>1</sup>, Zhong-Hao Jiang<sup>1,2</sup>, Yan-Yan Yi<sup>1</sup>, Yi Yang<sup>1</sup>, Li-Ping Ke<sup>3</sup>, Zhen-Ming Pei<sup>1,2</sup> and Shan Zhu<sup>1\*</sup>

<sup>1</sup> College of Life and Environmental Sciences, Hangzhou Normal University, Hangzhou, China, <sup>2</sup> Department of Biology, Duke University, Durham, NC, USA, <sup>3</sup> Key Laboratory of Plant Secondary Metabolism and Regulation of Zhejiang Province, College of Life Sciences, Zhejiang Sci-Tech University, Hangzhou, China

To survive, plants must respond rapidly and effectively to various stress factors, including biotic and abiotic stresses. Salinity stress triggers the increase of cytosolic free  $\text{Ca}^{2+}$  concentration ( $[\text{Ca}^{2+}]_i$ ) via  $\text{Ca}^{2+}$  influx across the plasma membrane, as well as bacterial flg22 and plant endogenous peptide Pep1. However, the interaction between abiotic stress-induced  $[\text{Ca}^{2+}]_i$  increases and biotic stress-induced  $[\text{Ca}^{2+}]_i$  increases is still not clear. Employing an aequorin-based  $\text{Ca}^{2+}$  imaging assay, in this work, we investigated the  $[\text{Ca}^{2+}]_i$  changes in response to flg22, Pep1, and NaCl treatments in *Arabidopsis thaliana*. We observed an additive effect on the  $[\text{Ca}^{2+}]_i$  increase which induced by flg22, Pep1, and NaCl. Our results indicate that biotic and abiotic stresses may activate different  $\text{Ca}^{2+}$  permeable channels. Further, calcium signal induced by biotic and abiotic stresses was independent in terms of spatial and temporal patterning.

**Keywords:** biotic stress, abiotic stress, flg22, Pep1, aequorin-based  $\text{Ca}^{2+}$  imaging, calcium signal

## OPEN ACCESS

### Edited by:

Qi Xie,  
Institute of Genetics and  
Developmental Biology (CAS), China

### Reviewed by:

YeonKyeong Lee,  
Norwegian University of Life Sciences,  
Norway  
Gang Li,  
University of Nebraska-Lincoln, USA

### \*Correspondence:

Shan Zhu  
szhu@hznu.edu.cn

### Specialty section:

This article was submitted to  
Plant Physiology,  
a section of the journal  
Frontiers in Plant Science

**Received:** 15 November 2016

**Accepted:** 16 January 2017

**Published:** 31 January 2017

### Citation:

Cao X-Q, Jiang Z-H, Yi Y-Y, Yang Y,  
Ke L-P, Pei Z-M and Zhu S (2017)  
Biotic and Abiotic Stresses Activate  
Different  $\text{Ca}^{2+}$  Permeable Channels  
in *Arabidopsis*. *Front. Plant Sci.* 8:83.  
doi: 10.3389/fpls.2017.00083

## INTRODUCTION

In the natural environment, plants have to continuously cope with various stress factors, such as salt, drought, attacks of herbivorous insects, and invasion of microbial pathogens. To survive, plants should respond rapidly and effectively to each stressor. Recent studies revealed that about 10 million hectares of agricultural land are abandoned every year due to high salinity (Zhu, 2001, 2003; Munns and Tester, 2008). Plant diseases cause massive losses in agricultural yields as well as abiotic stresses (Singh et al., 2011; Dangl et al., 2013; Yoshida et al., 2013). Moreover, the simultaneous occurrence of different stresses results in a high degree of complexity in terms of plant responses, as the responses to the combined stresses are largely controlled by different, and sometimes opposing, signaling pathways that may interact and inhibit each other (Suzuki et al., 2014). Therefore, it is critical to study how plants respond to both biotic and abiotic stresses.

The calcium, which serves as a secondary messenger, is thought to be a key element in plants to understand how a sophisticated network of signaling pathways respond to various abiotic and biotic stimuli (Hetherington and Brownlee, 2004; Pandey et al., 2004; Dodd et al., 2010; Yuan et al., 2014). The calcium ( $\text{Ca}^{2+}$ ) signaling has been implicated in regulating many perspectives of plant growth and responses to the environment (McAinsh and Pittman, 2009; Dodd et al., 2010; Kudla et al., 2010). Immunity of plant activates two signal transduction pathways, i.e.,  $\text{Ca}^{2+}$  signaling pathways and cytoplasmic mitogen-activated protein kinase, thus leading to transcriptional reprogramming and accumulation of chloroplast-derived reactive oxygen species (ROS; Zhang et al., 2007; Boudsocq et al., 2010; Dubiella et al., 2013;

Li et al., 2014) as well as generation of defense-related hormones, e.g., jasmonic acid and salicylic acid (Grant and Jones, 2009; Klauser et al., 2015). Abiotic stress also triggers a calcium-signaling cascade in plants, leading to transcriptional regulation and subsequent physiological as well as developmental responses. Salt stress is a representative of such abiotic stresses. Although the molecular mechanisms surrounding the initial perception of salt stress are unknown, it is now well established that salt stress triggers a transient increase in cytosolic  $\text{Ca}^{2+}$  concentration ( $[\text{Ca}^{2+}]_i$ ) that lasts for approximately 2 min (Knight et al., 1997; Tracy et al., 2008; Jiang et al., 2013).

These specific  $\text{Ca}^{2+}$  signatures are formed as a result of the tightly regulated activities of  $\text{Ca}^{2+}$  channels and transporters in different tissues, organelles, and membranes (Rentel and Knight, 2004; Kudla et al., 2010; Spalding and Harper, 2011; Batistic and Kudla, 2012; Stael et al., 2012). In terms of plant immunity, the changes of  $[\text{Ca}^{2+}]_i$  are detected by cytosolic  $\text{Ca}^{2+}$  sensors. One of the earliest signaling events following the perception of microbe-associated molecular patterns (MAMPs) or damage-associated molecular patterns (DAMPs) is a rapid change of  $[\text{Ca}^{2+}]_i$  and concomitant membrane depolarization (Blume et al., 2000; Lecourieux et al., 2002; Ranf et al., 2008; Jeworutzki et al., 2010; Nomura et al., 2012; Li et al., 2014). Consequently, the generation of ROS could restrict the growth of pathogen via cell wall strengthening and toxic effects, or initiate signaling functions (Torres et al., 2002; Chinchilla et al., 2007; Ranf et al., 2011; Kadota et al., 2015). As the first line of innate immunity, pattern-recognition receptors (PRRs) can recognize MAMPs in the plasma membrane and trigger a series of basal defense responses (Macho and Zipfel, 2014; Yamada et al., 2016). Plant nucleotide-binding and leucine-rich repeat (NB-LRR) proteins, encoded by plant “R” genes, recognize pathogen-derived effector proteins and trigger hypersensitive response (Tsuda and Katagiri, 2010; Zipfel, 2014). The well-studied pathogen-associated molecular pattern (PAMP)/PRR pairs in *Arabidopsis* so far are EF-Tu/EFR (elongation factor thermo unstable receptor) and flagellin/FLS2 (flagellin-sensitive 2), with the peptides elf18 and flg22, respectively, functioning as the elicitor-active PAMPs (Felix et al., 1999; Gomez-Gomez et al., 1999; Gomez-Gomez and Boller, 2000; Kunze et al., 2004; Zipfel et al., 2006). Other biotic stresses, as well as Pep1, a plant-derived DAMP, have been reported in recent years (Huffaker et al., 2006; Huffaker and Ryan, 2007; Shan et al., 2008; Krol et al., 2010).

From recent studies, we know that both biotic and abiotic stresses can trigger a rapid increase in cytosolic  $\text{Ca}^{2+}$ . Jiang et al. (2013) reported that NaCl-gated  $\text{Ca}^{2+}$  channels and  $\text{H}_2\text{O}_2$ -gated  $\text{Ca}^{2+}$  channels may differ. This study also suggests that NaCl- and  $\text{H}_2\text{O}_2$ -evoked  $[\text{Ca}^{2+}]_i$  may reduce the potency of both NaCl and  $\text{H}_2\text{O}_2$  in triggering  $[\text{Ca}^{2+}]_i$  increases, highlighting the existence of a feedback mechanism. Alternatively, NaCl and  $\text{H}_2\text{O}_2$  may activate the same  $\text{Ca}^{2+}$  permeable channel, which is expressed in different types of cells and/or activated via different signaling pathways. However, it is still not clear whether biotic and abiotic stress-activated  $\text{Ca}^{2+}$  channels influence each other or they are independent of each other. Moreover, the activation of  $\text{Ca}^{2+}$  channels by different biotic stresses (e.g., MAMP/DAMP) is a topic, which is also worthy of investigation.

In this study, we systematically investigated and analyzed the relationship and interaction between biotic and abiotic stresses in *Arabidopsis*. We found that the increases of  $[\text{Ca}^{2+}]_i$  induced by both stimuli were higher than those induced by a single stress, suggesting that biotic and abiotic stresses have an additive effect on  $[\text{Ca}^{2+}]_i$ . We also found that flg22-induced  $[\text{Ca}^{2+}]_i$  increases may inhibit both PAMP- and DAMP-activated  $[\text{Ca}^{2+}]_i$  channels via a feedback mechanism, but not abiotic-activated  $[\text{Ca}^{2+}]_i$  channels. These results suggest that the responses involve in both inhibitory feedback mechanisms, as well as an interaction between the stimuli-mediated  $\text{Ca}^{2+}$  signaling pathways.

## MATERIALS AND METHODS

### Plant Materials and Growth Conditions

*Arabidopsis thaliana* ecotype Col-0 constitutively expressing intracellular  $\text{Ca}^{2+}$  indicator aequorin (pMAQ2) is a gift from M. Knight and the principles of how the active aequorin is formed can be found in Knight et al. (1991). *Arabidopsis* plants were grown in 150 mm × 15 mm round Petri dishes in half-strength Murashige and Skoog salts (MS; Gibco), supplemented with 1.5% (w/v) sucrose (Sigma), and 0.8% (w/v) agar (Becton Dickinson) adjusted to pH 6.0 with KOH in controlled an environmental room at  $21 \pm 2^\circ\text{C}$ . The fluency rate of white light was  $\sim 110 \mu\text{mol m}^{-2} \text{s}^{-1}$ . The photoperiods were 16 h light/8 h dark cycles. Seeds were sterilized with 2.5% plant preservative mixture (Caisson Laboratories) and stratified at  $4^\circ\text{C}$  for 3 days in the dark, and then transferred to the growth room.

### Aequorin Reconstitution and Measurement of $[\text{Ca}^{2+}]_i$

*Arabidopsis thaliana* plants expressing cytosolic apoaequorin were used for  $[\text{Ca}^{2+}]_i$  measurements (Knight et al., 1991; Tang et al., 2007). Sixty-four seedlings were grown on half-strength MS medium for 8 days. Reconstitution of aequorin was performed *in vivo* by spraying seedlings with 3.3 mL of 10  $\mu\text{M}$  coelenterazine (from Prolume) per Petri dish followed by incubation at  $22^\circ\text{C}$  in the dark for 8 h. Treatments and aequorin luminescence imaging were performed at room temperature using a ChemiPro HT system, which includes a cryogenically cooled and back-illuminated charge-coupled device (CCD) camera, liquid nitrogen autofiller, camera controller, and computer-equipped WinView/32 software (Roper Scientific) as described previously (Tang et al., 2007). The CCD camera has a  $1300 \times 1340$  pixel resolution and is cooled to  $-120^\circ\text{C}$  by the cryogenic cooler system prior to image recording. The recording was started 80 s prior treatments and luminescence images were taken every 20 s or continuous 7 min. The total remaining aequorin was estimated by treating plants with a discharging solution containing 0.9 M  $\text{CaCl}_2$  in 10% (v/v) ethanol and recorded for 5 min until values were within 1% of the highest discharge value (Tang et al., 2007; Ranf et al., 2012; Yuan et al., 2014). The recorded luminescence images were analyzed using Meta Morph 7.7 and WinView/32. Here, the  $\text{Ca}^{2+}$  level depicted as  $L/L_{max}$  ratio correlates with the light emission from aequorin. To calculate the ratio, the actual aequorin luminescence, denoted

as  $L$ , at any sampling point is normalized by the total remaining aequorin (Knight et al., 1996; Ranf et al., 2012). The experiments were carried out under room temperature between 22 and 24°C.

## Elicitors and NaCl Treatments

For stress treatments, Petri dishes were placed individually into the ChemiPro HT chamber and luminescence images were started 80 s prior the treatment and taken at 20 s intervals or 7 min continuously. The treatment solution (100 mL) at 1  $\mu$ M concentrations of flg22 and Pep1 (Felix et al., 1999; Huffaker et al., 2006), which were synthesized by China Peptide<sup>1</sup> or 200 mM NaCl (Sigma) was added into Petri dish in the dark, and luminescence was recorded. For changes in bath solution, a four-channel peristaltic pump (Dynamax RP-1, Rainin) was used to perfuse Petri dish with water as indicated in the figures. Then, additional stress treatment was applied by adding 100 mL solution into Petri dish.

## RESULTS

### Dose-Dependence and Kinetics of flg22- and Pep1-Induced $[Ca^{2+}]_i$ Increases

Changes in cytosolic  $Ca^{2+}$  concentration ( $[Ca^{2+}]_i$ ) can be monitored by the bioluminescent  $Ca^{2+}$ -binding protein aequorin *in vivo* (Knight et al., 1991). Apoaequorin can be expressed in plants and spontaneously reconstitutes to functional holo-aequorin upon addition of the native luminophore coelenterazine (CTZ-n) or chemically modified derivatives, such as coelenterazine-h (CTZ-h), for enhanced sensitivity (Shimomura et al., 1993; Mithofer and Mazars, 2002).

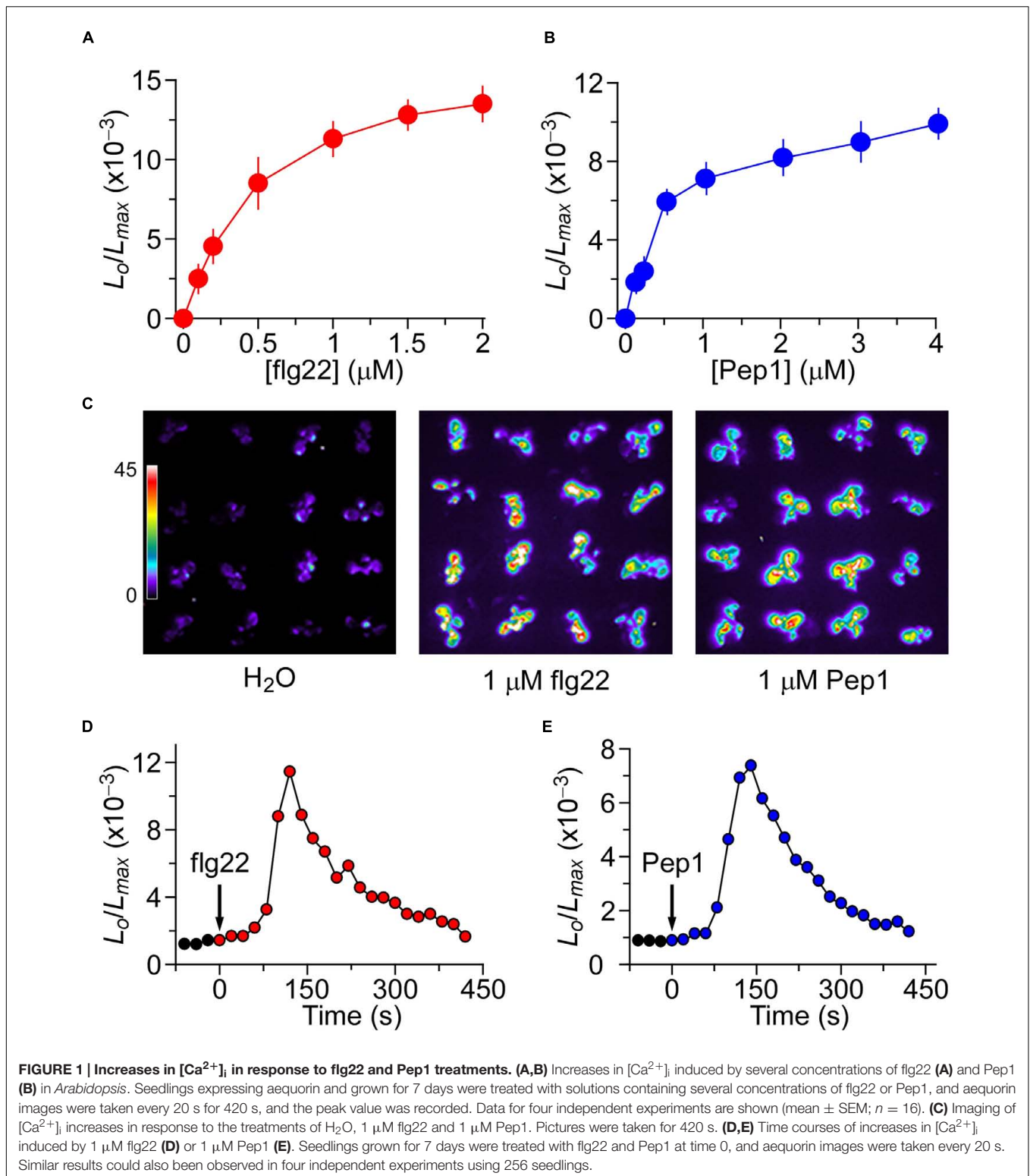
To determine whether the mechanisms behind the increases of  $[Ca^{2+}]_i$  induced by biotic and abiotic stresses are interrelated in *Arabidopsis*, we first attempted to identify the optimum concentrations of flg22 and Pep1 that ideally could be applied to generate about half of the maximum amplitude of  $[Ca^{2+}]_i$  required for potential up- and down-regulation. Furthermore, we attempted to establish the kinetics of flg22- and Pep1-induced  $[Ca^{2+}]_i$  increases so as to administer these stresses in different sequential combinations. To analyze flg22-induced increases in  $[Ca^{2+}]_i$ , we treated *Arabidopsis* seedlings expressing aequorin with solutions containing 0 to 2  $\mu$ M flg22. Aequorin bioluminescence images were recorded every 20 s for 600 s. The  $Ca^{2+}$  level correlates with the light emission from aequorin and is depicted as the ratio of  $L/L_{max}$ , where the actual aequorin luminescence ( $L$ ) at any measurement point is normalized to the total remaining aequorin (Knight et al., 1996). Plants grown on the half-strength MS medium had an average basal  $[Ca^{2+}]_i$  of  $80 \pm 21$  nM (Dodd et al., 2010). As expected, the  $[Ca^{2+}]_i$  increased in response to flg22 treatment (Figure 1A). The magnitudes of  $[Ca^{2+}]_i$  increases were found to be dependent on the concentration of flg22, with a higher concentration of flg22 evoking a greater increase in  $[Ca^{2+}]_i$ . The flg22 concentration required for a half-maximal response (i.e., the half of elicitor concentration which induced maximal  $[Ca^{2+}]_i$  increase) was

1  $\mu$ M, which was chosen as an optimum concentration for the subsequent analysis of interaction with Pep1- and NaCl-induced increases in  $[Ca^{2+}]_i$ . Next, we determined the temporal dynamics of flg22-induced  $[Ca^{2+}]_i$  increases under the imposed experimental conditions as a control for further comparison (Figure 1D). We found that  $[Ca^{2+}]_i$  increased immediately after the application of 1  $\mu$ M flg22, reached a peak at about 120 s, and then declined gradually (Figure 1D). Imaging aequorin bioluminescence for less than 20 s resulted in images with a low signal-noise ratio in our system. Thus, the temporal resolution was set at about 20 s, which was sufficient for the current study. At about 200 s, the  $[Ca^{2+}]_i$  was reduced to a new resting level. Similarly, we analyzed the increases in  $[Ca^{2+}]_i$  in response to Pep1. Seedlings were treated with different concentrations of Pep1 from 0 to 4  $\mu$ M, and  $[Ca^{2+}]_i$  was analyzed. As expected, Pep1 induced increases in  $[Ca^{2+}]_i$  in a dose-dependent manner (Figure 1B). The  $[Ca^{2+}]_i$  increases recorded after single treatments were consistent with the results described above (Figure 1C). The Pep1 concentration required to achieve a half-maximal response was around 1  $\mu$ M, with the magnitude of  $[Ca^{2+}]_i$  similar to that induced by 1  $\mu$ M flg22. We then determined the temporal dynamics of the  $[Ca^{2+}]_i$  increase induced by 1  $\mu$ M Pep1. Following treatment with 1  $\mu$ M Pep1, the  $[Ca^{2+}]_i$  increased and reached a peak at 140 s (Figure 1E), then it took another 250 s for the  $[Ca^{2+}]_i$  to reach a new basal level. In overall, it seems that the increases of  $[Ca^{2+}]_i$  occur faster in response to flg22 than Pep1, but reset to a resting level 400 s after the treatment.

### The Crosstalk between flg22- and Pep1-Induced $[Ca^{2+}]_i$ Increases

To further characterize the potential interaction between the different biotic stress stimuli-triggered  $[Ca^{2+}]_i$  signaling, plants were treated either with the same or different stimulus. When the *Arabidopsis* seedlings were treated with 1  $\mu$ M flg22, the level of  $[Ca^{2+}]_i$  increased quickly to reach a peak, then decreased to the new resting level after 400 s (Figure 2A), as described in Figure 1A. A subtle increase in  $[Ca^{2+}]_i$  could be detected in seedlings after they had been washed with deionized water at around 500 s (Figure 2A; green). Next, flg22 was added again, which resulted in a very minor increase in  $[Ca^{2+}]_i$ . After 800 s, it decayed to a level similar to the previous resting level. Compared with the first flg22 treatment, which led to a large  $[Ca^{2+}]_i$  increase, the second flg22 treatment resulted in a  $[Ca^{2+}]_i$  increase that was only a fraction of the size of the first  $[Ca^{2+}]_i$  increase. This observation suggests that the flg22-activated  $Ca^{2+}$  permeable channel may be desensitized or adapted by some unknown signaling elements upstream. To test whether the desensitization or adaptation occurs, we can (after waiting for 3 h) detect a normal  $[Ca^{2+}]_i$  increase in response to flg22. This result suggests that desensitization of the channel is likely to happen, which agrees with the results reported by Heese's group (Smith et al., 2014). Subsequently, we analyzed whether the MAMP-activated  $Ca^{2+}$  permeable channel was affected by the initial MAMP treatment. The second flg22 treatment was replaced by a treatment with 1  $\mu$ M Pep1 at 600 s (Figure 2B). Interestingly, the peak of  $[Ca^{2+}]_i$  induced by 1  $\mu$ M Pep1 was clearly greater

<sup>1</sup><http://www.chinapeptides.net>



than that of 1  $\mu$ M flg22 ( $P < 0.001$ ). After 900 s, the  $[Ca^{2+}]_i$  decreased to a new basal level (Figure 2B). The lower inhibition of the Pep1-induced  $[Ca^{2+}]_i$  increase compared with the increase induced by the initial flg22 treatment suggests that the initial

high level of  $[Ca^{2+}]_i$ , which resulted from the flg22 treatment, inhibited flg22 to a greater extent than Pep1 (Figures 2A,B). By analogy, we used Pep1 as the first stimulus to treat the seedlings, and then analyzed the second treatment using flg22 or Pep1.

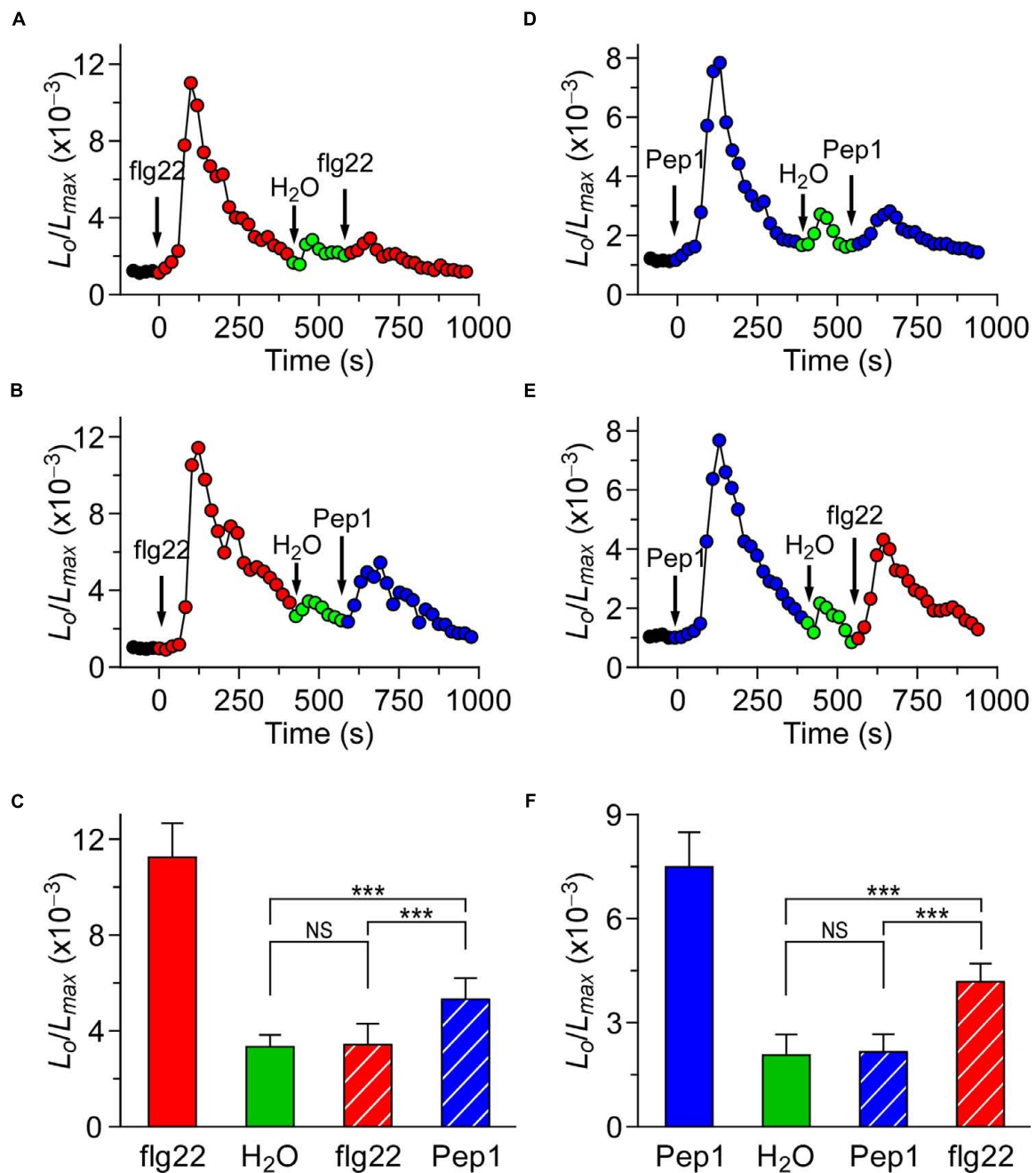
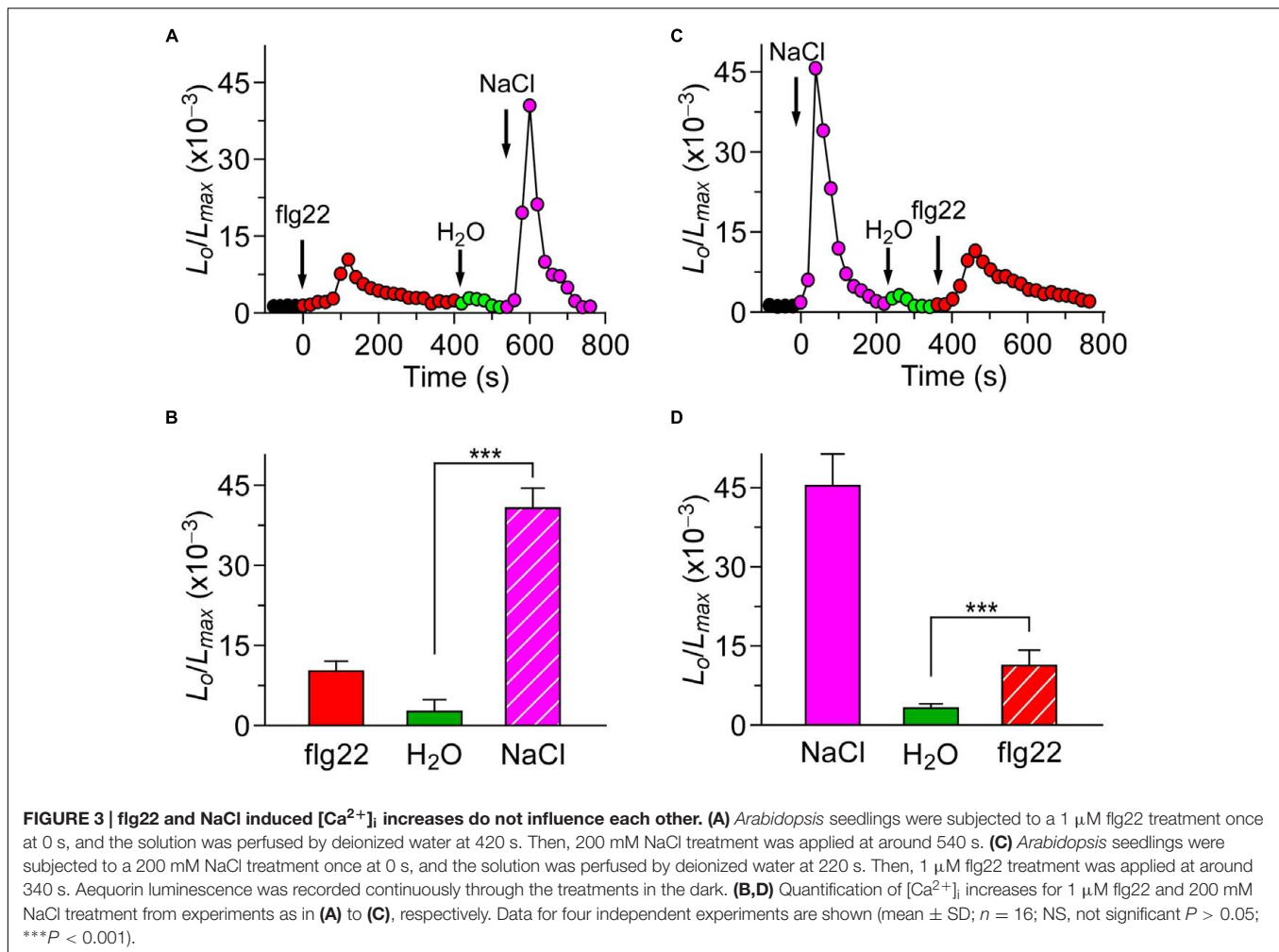


**FIGURE 2 | flg22 and Pep1 induced  $[Ca^{2+}]_i$  increases partly influence each other. (A,B)** *Arabidopsis* seedlings were subjected to a 1  $\mu$ M flg22 treatment once at 0 s, and the solution was perfused by deionized water at 420 s. Then, a second 1  $\mu$ M flg22 (A), or 1  $\mu$ M Pep1 (B) treatment was applied at around 540 s. (D,E) *Arabidopsis* seedlings were subjected to a 1  $\mu$ M Pep1 treatment once at 0 s, and the solution was perfused by deionized water at 420 s. Then, a second 1  $\mu$ M Pep1 (D), or 1  $\mu$ M flg22 (E) treatment was applied at around 540 s. Aequorin luminescence was recorded continuously through the treatments in the dark. (C,F) Quantification of  $[Ca^{2+}]_i$  increases for 1  $\mu$ M flg22 and 1  $\mu$ M Pep1 treatment from experiments as in (A) to (B), and (D) to (E), respectively. Data for four independent experiments are shown (mean  $\pm$  SD;  $n = 16$ ; NS, not significant  $P > 0.05$ ; \*\*\* $P < 0.001$ ).

When the second Pep1 was added to the Petri dish, following the first Pep1 treatment and water washing step at around 540 s the  $[Ca^{2+}]_i$  level stabilized to a point similar to previous resting levels (Figures 2D,E). The column chart has also been used to

clearly show the results, as in Figures 2C,F. However, when we used 1  $\mu$ M flg22 to replace Pep1 at 600 s, the peak value was smaller but significantly higher than that induced by the second Pep1 treatment (Figures 2D,E). Similarly, our results suggested



that the high  $[Ca^{2+}]_i$  resulting from the initial Pep1 activation inhibited the MAMP-induced  $[Ca^{2+}]_i$  to a greater degree than the PAMP-induced  $[Ca^{2+}]_i$  (Figure 2).

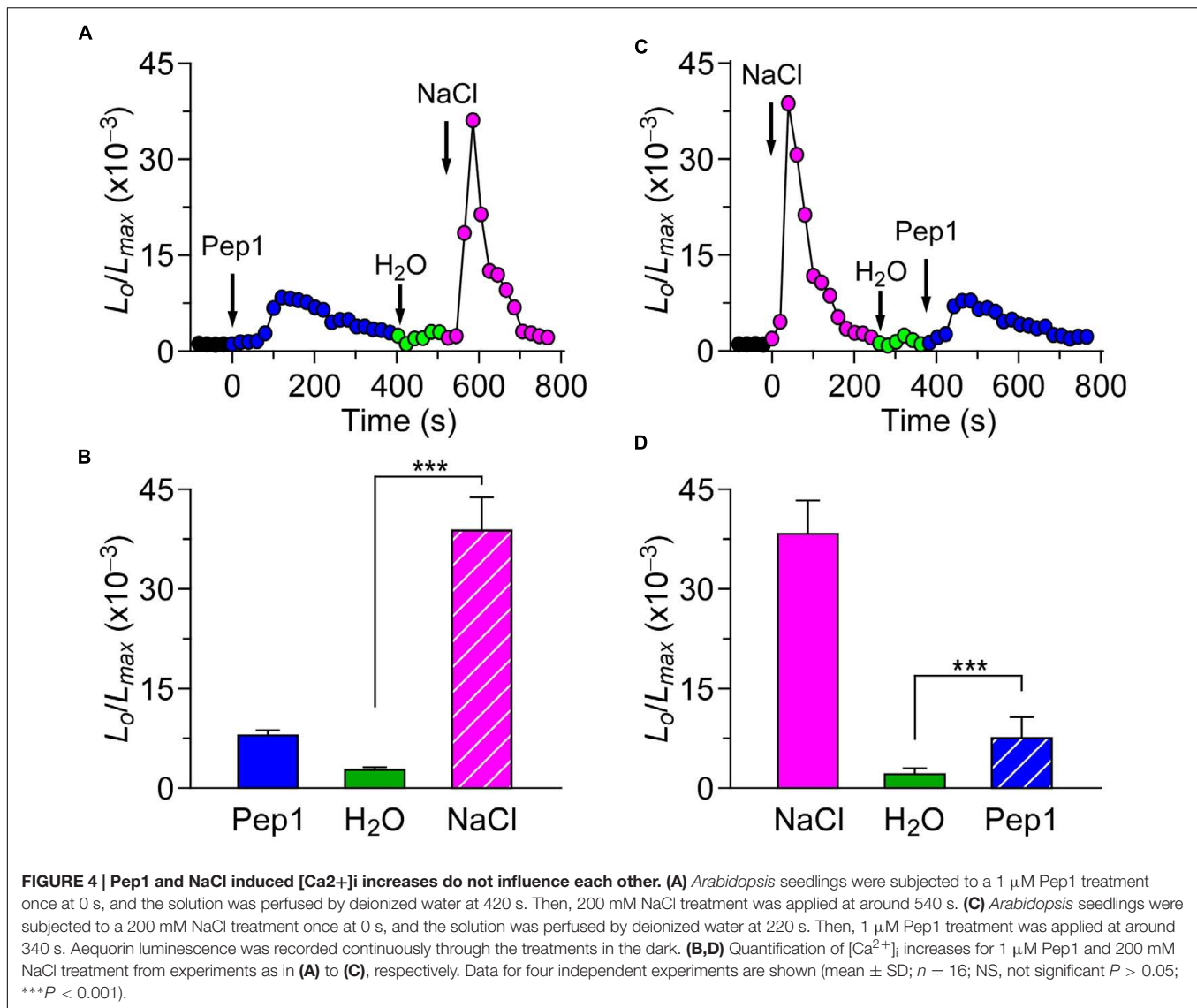
### The Crosstalk between Biotic and Abiotic Stresses-Triggered $[Ca^{2+}]_i$ Increases

Based on our study, we know that different biotic stresses may induce  $[Ca^{2+}]_i$  increases via different channels. It is of great importance to further characterize the interaction between biotic and abiotic stress stimuli-triggered  $[Ca^{2+}]_i$  signaling. For such a purpose, we treated the plants with both the biotic and abiotic stimulus. When the *Arabidopsis* seedlings were treated with 1  $\mu$ M flg22, the level of  $[Ca^{2+}]_i$  increased rapidly to reach a peak, and decreased to the new resting level after 400 s. A subtle increase in  $[Ca^{2+}]_i$  could be detected in the seedlings after they were washed in deionized water at around 500 s (Figure 3A; green). Next, NaCl was added, which caused a sharp increase in  $[Ca^{2+}]_i$  (Figure 3A). The  $[Ca^{2+}]_i$  then decayed from 700 s to a level similar to previous resting level. Compared with the single NaCl treatment, which led to a large increase in  $[Ca^{2+}]_i$  increase (Figure 3C), the NaCl treatment after the flg22 stimulus

still resulted in an increase in  $[Ca^{2+}]_i$  that was similar to a single NaCl-induced increase in  $[Ca^{2+}]_i$ . This observation suggests that there may be no interaction between the NaCl-activated  $Ca^{2+}$  permeable channel (NaC) and flg22-activated  $Ca^{2+}$  permeable channel. To verify this hypothesis, we treated the seedlings with 200 mM NaCl. The  $[Ca^{2+}]_i$  increased quickly to reach a peak and then decreased to the new resting level after 150 s (Figure 3C). Next, we added 1  $\mu$ M of flg22, which caused an increase in  $[Ca^{2+}]_i$  similar to the effect with a single flg22 treatment. Subsequently, we used a DAMP elicitor Pep1 instead of flg22 to determine whether a DAMP-induced  $[Ca^{2+}]_i$  increase can affect an NaC. To clearly show the results, column charts were used in Figures 3B,D. As expected, it appeared that there was no interaction between the NaC and Pep1-activated  $Ca^{2+}$  permeable channel (Figures 3A–D). Based on this study, our results suggest that abiotic and biotic stress stimuli-activated  $Ca^{2+}$  permeable channels may be completely independent of each other.

### The Additive Effect of flg22, Pep1, and NaCl on Triggering Increases in $[Ca^{2+}]_i$

To investigate thoroughly the relationship and interaction between  $[Ca^{2+}]_i$  increases triggered by biotic and abiotic stresses,

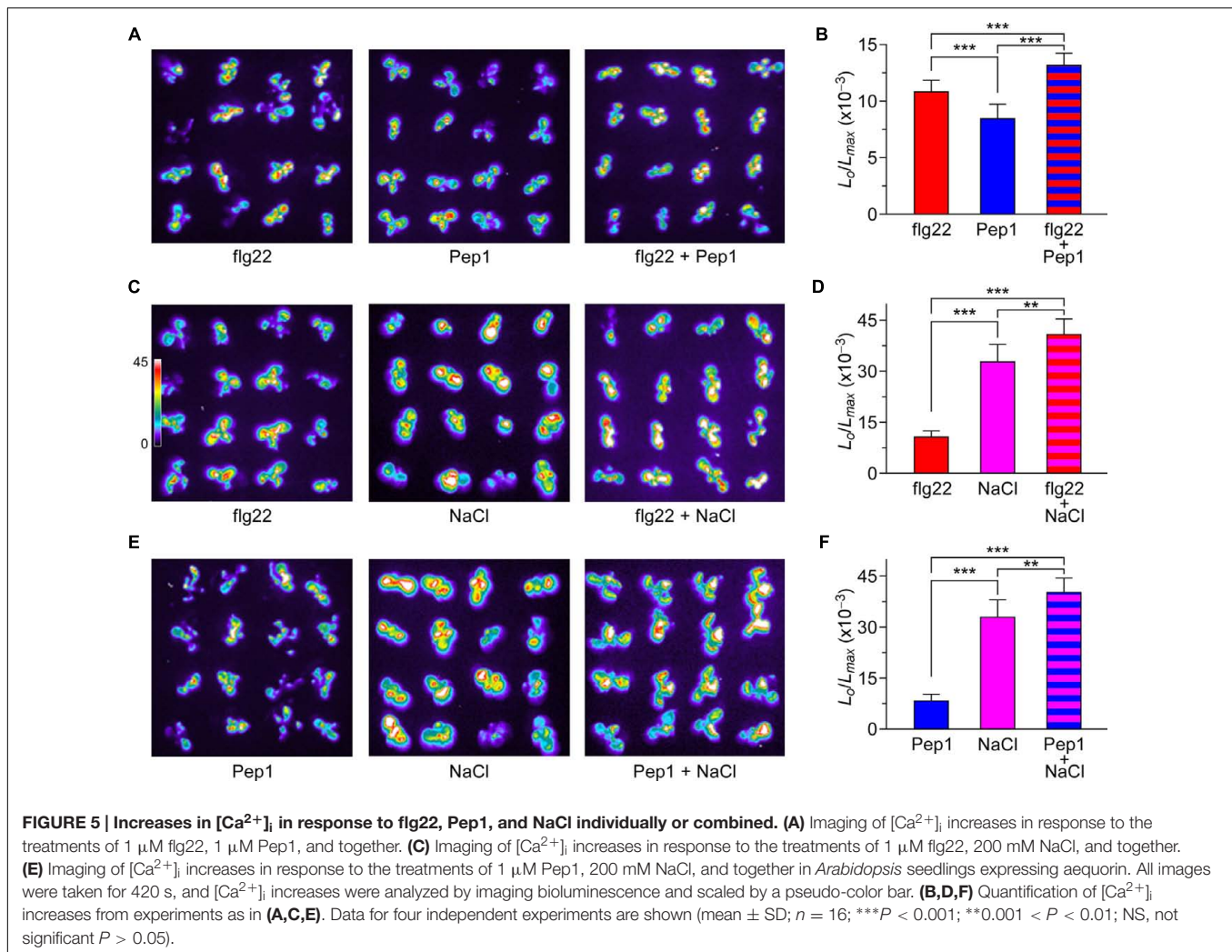


*Arabidopsis* seedlings were treated with 1  $\mu$ M flg22, 1  $\mu$ M Pep1, or 200 mM NaCl separately, or any two of these three elicitors. The  $[Ca^{2+}]_i$  increases recorded after single treatments were consistent with the results described above. When plants were treated with 1  $\mu$ M flg22 and 1  $\mu$ M Pep1 together, the peaks of  $[Ca^{2+}]_i$  were slightly larger than those induced by each individual stimulus (Figure 5A). However, when plants were treated with 200 mM NaCl together with 1  $\mu$ M flg22 or 1  $\mu$ M Pep1, the peaks of  $[Ca^{2+}]_i$  were larger than those induced by each individual stimulus, showing an additive effect (Figures 5C,E). To further analyze the difference in  $[Ca^{2+}]_i$  increases in response to both biotic and abiotic stresses, we calculate the  $[Ca^{2+}]_i$  to clearly illustrate the data. As shown in Figure 5B, compared with individual treatment with Pep1, plants treated with flg22 and Pep1 together show only a slight increase in  $[Ca^{2+}]_i$ . However, compared with individual treatment with NaCl, plants treated with flg22 and NaCl together, or Pep1 and NaCl together, show an increase in  $[Ca^{2+}]_i$  that

is almost equal to that shown with the combined treatment (Figures 5D,F). These results suggest that the flg22-induced and Pep1-induced  $[Ca^{2+}]_i$  increases may operate through similar  $Ca^{2+}$  permeable channels, though biotic stress-induced  $[Ca^{2+}]_i$  increases may occur as independent events. In other words, biotic and abiotic stresses may activate different  $Ca^{2+}$  permeable channels.

### Calcium Signaling Induced by Biotic and Abiotic Stresses Are Independent in Terms of Spatial and Temporal Patterning

The co-treatment of biotic and abiotic stresses triggers an additive effect on the increase of  $[Ca^{2+}]_i$ . Treated either by flg22 with NaCl or Pep1 with NaCl, the increase of  $[Ca^{2+}]_i$  could indicate that biotic and abiotic stresses activate different  $Ca^{2+}$  permeable channels. While it is not clear whether the treatment of NaCl will



affect the calcium signal process and peak value, which are caused by the flg22/Pep1 treatment. To answer this question, in our experiments, seedlings were treated either by 1  $\mu$ M flg22 along with 200 mM NaCl or 1  $\mu$ M Pep1 along with 200 mM NaCl. The results are shown in **Figure 6**. The shaded area in **Figures 6A,D** illustrates the difference between the co-treated plants and NaCl-only treated plants. The subtracted shaded area reveals that the dynamic process and peak value of  $[Ca^{2+}]_i$  achieved by the treatment of using both flg22 and Pep1 are similar to those delivered by using the flg22 or Pep1 alone (**Figures 6B,C,E,F**). These results indicate that biotic and abiotic stresses induce the increase of  $[Ca^{2+}]_i$  through different  $Ca^{2+}$  permeable channels. Such results are consistent with our prediction.

## DISCUSSION

Calcium is the most important secondary messenger and plays an essential role in signal transduction throughout the lives of both animals and plants (Berridge et al., 2003; Clapham, 2007; Ward et al., 2009; Ranf et al., 2011). Changes in  $[Ca^{2+}]_i$  in response to

various abiotic and biotic stresses (including pathogen elicitors, salt stress, drought stresses, oxidative stress, and high and low temperatures) in plants have been a topic of much interest over the past two decades (McAinsh and Pittman, 2009; Dodd et al., 2010; Ma and Berkowitz, 2011; Yuan et al., 2014). Specific stimuli can trigger unique temporal and spatial patterns of  $[Ca^{2+}]_i$  known as " $[Ca^{2+}]_i$  signatures" (Tang et al., 2007; Spalding and Harper, 2011). The  $[Ca^{2+}]_i$  signature encodes information from the environmental stimulus which will be decoded subsequently by intracellular  $Ca^{2+}$  sensors, such as calcium-dependent protein kinases, calmodulins, and calcineurin B-like proteins, leading to the activation of downstream events (Galon et al., 2008; Jeworutzki et al., 2010; Stael et al., 2012; Steinhorst and Kudla, 2013; Seybold et al., 2014). Basal  $[Ca^{2+}]_i$  is controlled below the extracellular  $Ca^{2+}$  concentration at a concentration round 10,000-fold (Berridge et al., 2003; Clapham, 2007; Swanson et al., 2011). Generally, in response to environmental stimuli,  $Ca^{2+}$  channels in the plasma membrane and/or endomembranes can be activated and lead to the increases of  $[Ca^{2+}]_i$  (Hetherington and Brownlee, 2004; Ward et al., 2009; Ranf et al., 2011). Biotic and abiotic stress-induced  $[Ca^{2+}]_i$  increases have traditionally

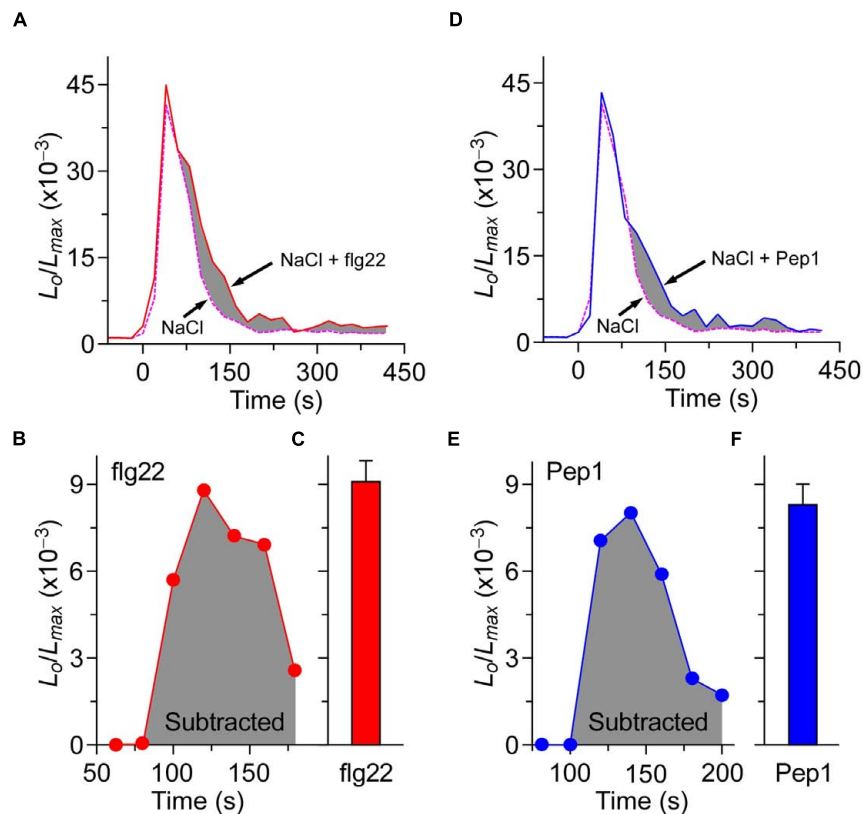


**FIGURE 6 | The processes of  $[Ca^{2+}]_i$  increases induced by biotic and abiotic stresses are independent. (A)** Time courses of increase in  $[Ca^{2+}]_i$  induced by 200 mM NaCl (dashed line) and 200 mM NaCl together with 1  $\mu$ M flg22 (full line). **(D)** Time courses of increase in  $[Ca^{2+}]_i$  induced by 200 mM NaCl (dashed line) and 200 mM NaCl together with 1  $\mu$ M Pep1 (full line). Seedlings grown for 7 days were treated at time 0, and aequorin images were taken every 20 s. **(B,C)** Increases in  $[Ca^{2+}]_i$  induced by 1  $\mu$ M flg22 that calculated from **(A)**. **(E,F)** Increases in  $[Ca^{2+}]_i$  induced by 1  $\mu$ M Pep1 that calculated from **(D)**. Similar results were seen in four independent experiments using 256 seedlings.

been considered to be involved in the procedure of perceiving the stress signaling, though the molecular nature of this process is poorly understood (Luan et al., 2009; Ranf et al., 2011). One recent study has shown that OSCA1 is a plasma membrane protein, which can be used to form hyperosmolality-gated calcium-permeable channels. This study reveals that OSCA1 could be served as an osmosensor. The OSCA1 represents a channel responsible for the increases of  $[Ca^{2+}]_i$  induced by a stimulus in plants, leading to a new avenue to study  $Ca^{2+}$  processes in relation to other stimuli (Yuan et al., 2014). Observing the lag phases and  $[Ca^{2+}]_i$  amplitudes in plant's early response, we found that  $[Ca^{2+}]_i$  increases induced by abiotic stresses are similar. Based on the above results we speculate that abiotic stress-induced  $[Ca^{2+}]_i$  signaling are mediated via a sensory channel. Thus, in contrast to abiotic stresses, the biotic stress-induced  $[Ca^{2+}]_i$  oscillation curve presents different lag phases and  $[Ca^{2+}]_i$  amplitudes. This demonstrates that both abiotic stress-induced and biotic stress-induced  $[Ca^{2+}]_i$  increases may utilize entirely different channels.

It is well known that recognition of PAMPs or DAMPs by PRRs leads to a first line of inducible defenses that restrict microbial propagation in multicellular organisms (Boller and

Felix, 2009; Gupta et al., 2011; Kawai and Akira, 2011; Segonzac and Zipfel, 2011; Zipfel, 2014; Bigeard et al., 2015; Yamada et al., 2016). Although it was reported many years ago that a rapid change in the cytosolic  $Ca^{2+}$  concentration ( $[Ca^{2+}]_i$ ) and concomitant membrane depolarization follows MAMP/DAMP perception, the interaction and interrelationship between many early MAMP/DAMP signaling components in *Arabidopsis* are not well understood. The lessening of the  $[Ca^{2+}]_i$  increases induced by both MAMPs and DAMPs observed in this study (**Figures 1D,E**) suggests that the feedback inhibitory mechanism could inactivate the stimulus-activated  $Ca^{2+}$  permeable channels. Briefly speaking, elevated  $[Ca^{2+}]_i$  will inhibit the ion channels in plants. We speculate that this phenomenon may be similar to the depolarization process of receptor ion channels typically seen in animals (Traynelis et al., 2010). One particular study reported that such receptor desensitization also occurs in plants (Smith et al., 2014). However, we did not observe any  $[Ca^{2+}]_i$  at 420 s after flg22 or Pep1 treatment (**Figures 1D,E**).

flg22 and Pep1 induced slightly increases of  $[Ca^{2+}]_i$  than using either flg22 or Pep1 alone (**Figure 5**), indicating that flg22 and Pep1 may, in part, share  $Ca^{2+}$  permeable channels flg22-C and Pep1-C (**Figure 7**). The flg22-C and Pep1-C are

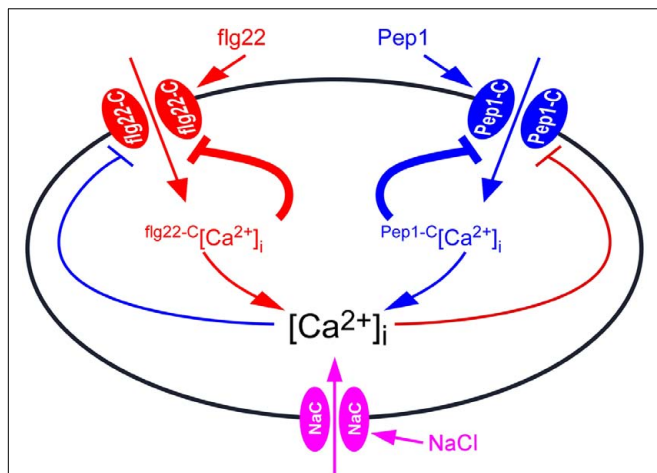


**FIGURE 7 | Model for the interaction between biotic and abiotic stresses-induced  $[Ca^{2+}]_i$  increases.**  $Ca^{2+}$  channel activated by flg22 (flg22-C) results in localized  $[Ca^{2+}]_i$  increases, called flg22-C-related  $[Ca^{2+}]_i$  microdomain (flg22-C $[Ca^{2+}]_i$ ). The flg22-C $[Ca^{2+}]_i$  feedback inhibits the activity of flg22-C. Pep1-C, a  $Ca^{2+}$  channel activated by hydrogen peroxide, leads to localized  $[Ca^{2+}]_i$  increases, called Pep1-C  $[Ca^{2+}]_i$  microdomain. Pep1-C  $[Ca^{2+}]_i$  also feedback inhibits Pep1-C activity. The  $[Ca^{2+}]_i$  microdomain-mediated inhibition of  $Ca^{2+}$  channels is the major feedback inhibitory pathways (thick lines). In addition, both flg22-C $[Ca^{2+}]_i$  and Pep1-C $[Ca^{2+}]_i$  might contribute to a NaCl-activated  $Ca^{2+}$  permeable channels (NaC), which further inhibits both flg22-C and Pep1-C, serving as biotic and abiotic stresses feedback inhibitory pathways (thin lines).  $[Ca^{2+}]_i$  is reset to the resting level by plasma membrane  $Ca^{2+}$  pumps.

likely regulated by feedback inhibition (Figure 7), considering their desensitization seen in this study (Figures 2A,D) as well as in previous reports. We demonstrated that repetitive flg22 treatments failed to trigger repetitive  $[Ca^{2+}]_i$  increases (Figures 2A,C). This indicates that the flg22-C cannot be activated repetitively within a short period of time—that is, flg22-C is possibly desensitized. We can therefore deduce that a feedback inhibition may be involved in the desensitization process (Figure 7). Upon flg22 treatment, the flg22-C opens, leading to a localized increase in  $[Ca^{2+}]_i$ , flg22-C  $[Ca^{2+}]_i$  microdomain/puff. The flg22-C  $[Ca^{2+}]_i$ , in turn, signals the channel to close, which prevents further  $[Ca^{2+}]_i$  increases and allows the basal  $[Ca^{2+}]_i$  to be reset via  $Ca^{2+}$  pumps. Such feedback inhibition avoids any excessive increase in  $[Ca^{2+}]_i$ , which could be highly deleterious to plant cells. The same phenomenon was also observed with the activation of Pep1-C (Figure 7). Clearly, the most significant effect was observed after the initial treatment by flg22-C or Pep1-C, when the rate of  $[Ca^{2+}]_i$  increases induced by both flg22-C and Pep1-C decreased (Figure 2). It is most probably that localized flg22-C  $[Ca^{2+}]_i$  and Pep1-C  $[Ca^{2+}]_i$  merge to form a obviously global  $[Ca^{2+}]_i$ , the feedback of which then inhibits both flg22-C and Pep1-C (Figure 5). In contrast, flg22 or Pep1, together with NaCl, induced greater increases in  $[Ca^{2+}]_i$  than using flg22 or Pep1 alone, leading us to conclude that there is no interrelationship between the NaCs. It should be noted that our study does not prove that flg22-C, Pep1-C, and NaC are localized in discrete and

different microdomains, instead illustrates that flg22-C, Pep1-C, and NaC may differ and interact via  $[Ca^{2+}]_i$  microdomains.

To some extent, PAMP- and DAMP-induced  $[Ca^{2+}]_i$  increases differ, but they all belong to the same pattern. In plants, biotic stresses that include PAMP- and DAMP-induced  $[Ca^{2+}]_i$  increases are similar in spatial and temporal patterning. Thus, we treated plants with flg22 together with Pep1, and found that the  $[Ca^{2+}]_i$  peaks were slightly larger than those induced by each stimulus alone, showing an enhanced signaling mechanism (Figure 5). This is similar to NaCl- and  $H_2O_2$ -induced  $[Ca^{2+}]_i$  increases (Jiang et al., 2013), suggesting that PAMPs and DAMPs may partly activate the same  $Ca^{2+}$  permeable channel. When plants were treated with NaCl together with flg22 or Pep1, the  $[Ca^{2+}]_i$  peaks were larger than those induced by each individual stimulus, showing an additive effect (Figures 5C,E). These results suggest that biotic and abiotic stresses may activate different  $Ca^{2+}$  permeable channels. In Figure 6, we present the calcium signal oscillation curve within the same image. We noticed that the calcium signal induced by biotic and abiotic stresses was independent in terms of spatial and temporal patterning. This study further demonstrates that early signaling is relatively independent to biotic and abiotic stresses.

Plants resist biotic and abiotic stresses by triggering two different sets of calcium signaling pathways. This is of great significance to the plant's survival strategies. It will be important for future research to analyze the pharmacological properties of these putative  $Ca^{2+}$  permeable channels activated by flg22. Clearly, identifying these channels or sensors is extremely important to study the plant stresses resistance. Additionally, how flg22-C and Pep1-C interact thus contributing to the development of  $[Ca^{2+}]_i$  signatures as well as other downstream events could be analyzed further once their molecular nature being revealed.

## AUTHOR CONTRIBUTIONS

SZ, Z-MP, and Z-HJ conceived and designed the experiments. X-QC, SZ, Y-YY, and YY performed the experiments. SZ, X-QC, and Z-MP analyzed the data. L-PK contributed reagents/materials/analysis tools. SZ wrote the manuscript.

## FUNDING

This work was financially supported by grants from the Zhejiang Provincial Natural Science Foundation of China (no. LQ14C020003). The National Natural Science Foundation of China (no. 31301170).

## ACKNOWLEDGMENTS

We thank Marc R. Knight for *Arabidopsis* seeds expressing aequorin, James N. Siedow for discussion and proof reading of the manuscript and the Pei lab members for discussion and support.

## REFERENCES

- Baticic, O., and Kudla, J. (2012). Analysis of calcium signaling pathways in plants. *Biochim. Biophys. Acta* 1820, 1283–1293. doi: 10.1016/j.bbagen.2011.10.012
- Berridge, M. J., Bootman, M. D., and Roderick, H. L. (2003). Calcium signalling: dynamics, homeostasis and remodelling. *Nat. Rev. Mol. Cell Biol.* 4, 517–529. doi: 10.1038/nrm1155
- Bigeard, J., Colcombet, J., and Hirt, H. (2015). Signaling mechanisms in pattern-triggered immunity (PTI). *Mol. Plant* 8, 521–539. doi: 10.1016/j.molp.2014.12.022
- Blume, B., Nurnberger, T., Nass, N., and Scheel, D. (2000). Receptor-mediated increase in cytoplasmic free calcium required for activation of pathogen defense in parsley. *Plant Cell* 12, 1425–1440. doi: 10.1105/tpc.12.8.1425
- Boller, T., and Felix, G. (2009). A renaissance of elicitors: perception of microbe-associated molecular patterns and danger signals by pattern-recognition receptors. *Annu. Rev. Plant Biol.* 60, 379–406. doi: 10.1146/annurev.arplant.57.032905.105346
- Boudsocq, M., Willmann, M. R., McCormack, M., Lee, H., Shan, L., He, P., et al. (2010). Differential innate immune signalling via Ca(2+) sensor protein kinases. *Nature* 464, 418–422. doi: 10.1038/nature08794
- Chinchilla, D., Zipfel, C., Robatzek, S., Kemmerling, B., Nurnberger, T., Jones, J. D., et al. (2007). A flagellin-induced complex of the receptor FLS2 and BAK1 initiates plant defence. *Nature* 448, 497–500. doi: 10.1038/nature05999
- Clapham, D. E. (2007). Calcium signaling. *Cell* 131, 1047–1058. doi: 10.1016/j.cell.2007.11.028
- Dangl, J. L., Horvath, D. M., and Staskawicz, B. J. (2013). Pivoting the plant immune system from dissection to deployment. *Science* 341, 746–751. doi: 10.1126/science.1236011
- Dodd, A. N., Kudla, J., and Sanders, D. (2010). The language of calcium signaling. *Annu. Rev. Plant Biol.* 61, 593–620. doi: 10.1146/annurev-arplant-070109-104628
- Dubiella, U., Seybold, H., Durian, G., Komander, E., Lassig, R., Witte, C. P., et al. (2013). Calcium-dependent protein kinase/NADPH oxidase activation circuit is required for rapid defense signal propagation. *Proc. Natl. Acad. Sci. U.S.A.* 110, 8744–8749. doi: 10.1073/pnas.1221294110
- Felix, G., Duran, J. D., Volko, S., and Boller, T. (1999). Plants have a sensitive perception system for the most conserved domain of bacterial flagellin. *Plant J.* 18, 265–276. doi: 10.1046/j.1365-313X.1999.00265.x
- Galon, Y., Nave, R., Boyce, J. M., Nachmias, D., Knight, M. R., and Fromm, H. (2008). Calmodulin-binding transcription activator (CAMTA) 3 mediates biotic defense responses in *Arabidopsis*. *FEBS Lett.* 582, 943–948. doi: 10.1016/j.febslet.2008.02.037
- Gomez-Gomez, L., and Boller, T. (2000). FLS2: an LRR receptor-like kinase involved in the perception of the bacterial elicitor flagellin in *Arabidopsis*. *Mol. Cell.* 5, 1003–1011. doi: 10.1016/S1097-2765(00)80265-8
- Gomez-Gomez, L., Felix, G., and Boller, T. (1999). A single locus determines sensitivity to bacterial flagellin in *Arabidopsis thaliana*. *Plant J.* 18, 277–284. doi: 10.1046/j.1365-313X.1999.00451.x
- Grant, M. R., and Jones, J. D. (2009). Hormone (dis)harmony moulds plant health and disease. *Science* 324, 750–752. doi: 10.1126/science.1173771
- Gupta, K. J., Fernie, A. R., Kaiser, W. M., and van Dongen, J. T. (2011). On the origins of nitric oxide. *Trends Plant Sci.* 16, 160–168. doi: 10.1016/j.tplants.2010.11.007
- Hetherington, A. M., and Brownlee, C. (2004). The generation of Ca(2+) signals in plants. *Annu. Rev. Plant Biol.* 55, 401–427. doi: 10.1146/annurev.arplant.55.031903.141624
- Huffaker, A., Pearce, G., and Ryan, C. A. (2006). An endogenous peptide signal in *Arabidopsis* activates components of the innate immune response. *Proc. Natl. Acad. Sci. U.S.A.* 103, 10098–10103. doi: 10.1073/pnas.0603727103
- Huffaker, A., and Ryan, C. A. (2007). Endogenous peptide defense signals in *Arabidopsis* differentially amplify signaling for the innate immune response. *Proc. Natl. Acad. Sci. U.S.A.* 104, 10732–10736. doi: 10.1073/pnas.0703343104
- Jeworutzki, E., Roelfsema, M. R., Anschutz, U., Krol, E., Elzenga, J. T., Felix, G., et al. (2010). Early signaling through the *Arabidopsis* pattern recognition receptors FLS2 and EFR involves Ca-associated opening of plasma membrane anion channels. *Plant J.* 62, 367–378. doi: 10.1111/j.1365-313X.2010.04155.x
- Jiang, Z., Zhu, S., Ye, R., Xue, Y., Chen, A., An, L., et al. (2013). Relationship between NaCl- and H<sub>2</sub>O<sub>2</sub>-induced cytosolic Ca<sup>2+</sup> increases in response to stress in *Arabidopsis*. *PLoS ONE* 8:e76130. doi: 10.1371/journal.pone.0076130
- Kadota, Y., Shirasu, K., and Zipfel, C. (2015). Regulation of the NADPH Oxidase RBOHD During Plant Immunity. *Plant Cell Physiol.* 56, 1472–1480. doi: 10.1093/pcp/pcv063
- Kawai, T., and Akira, S. (2011). Toll-like receptors and their crosstalk with other innate receptors in infection and immunity. *Immunity* 34, 637–650. doi: 10.1016/j.immuni.2011.05.006
- Klauser, D., Desurmont, G. A., Glauser, G., Vallat, A., Flury, P., Boller, T., et al. (2015). The *Arabidopsis* Pep-PEPR system is induced by herbivore feeding and contributes to JA-mediated plant defence against herbivory. *J. Exp. Bot.* 66, 5327–5336. doi: 10.1093/jxb/erv250
- Knight, H., Trewavas, A. J., and Knight, M. R. (1996). Cold calcium signaling in *Arabidopsis* involves two cellular pools and a change in calcium signature after acclimation. *Plant Cell* 8, 489–503. doi: 10.1105/tpc.8.3.489
- Knight, H., Trewavas, A. J., and Knight, M. R. (1997). Calcium signalling in *Arabidopsis thaliana* responding to drought and salinity. *Plant J.* 12, 1067–1078. doi: 10.1046/j.1365-313X.1997.12051067.x
- Knight, M. R., Campbell, A. K., Smith, S. M., and Trewavas, A. J. (1991). Transgenic plant aequorin reports the effects of touch and cold-shock and elicitors on cytoplasmic calcium. *Nature* 352, 524–526. doi: 10.1038/352524a0
- Krol, E., Mentzel, T., Chinchilla, D., Boller, T., Felix, G., Kemmerling, B., et al. (2010). Perception of the *Arabidopsis* danger signal peptide 1 involves the pattern recognition receptor AtPEPR1 and its close homologue AtPEPR2. *J. Biol. Chem.* 285, 13471–13479. doi: 10.1074/jbc.M109.097394
- Kudla, J., Baticic, O., and Hashimoto, K. (2010). Calcium signals: the lead currency of plant information processing. *Plant Cell* 22, 541–563. doi: 10.1105/tpc.109.072686
- Kunze, G., Zipfel, C., Robatzek, S., Niehaus, K., Boller, T., and Felix, G. (2004). The N terminus of bacterial elongation factor Tu elicits innate immunity in *Arabidopsis* plants. *Plant Cell* 16, 3496–3507. doi: 10.1105/tpc.104.026765
- Lecourieux, D., Mazars, C., Pauly, N., Ranjeva, R., and Pugin, A. (2002). Analysis and effects of cytosolic free calcium increases in response to elicitors in *Nicotiana glauca* cells. *Plant Cell* 14, 2627–2641. doi: 10.1105/tpc.005579
- Li, L., Li, M., Yu, L., Zhou, Z., Liang, X., Liu, Z., et al. (2014). The FLS2-associated kinase BIK1 directly phosphorylates the NADPH oxidase RbohD to control plant immunity. *Cell Host Microbe* 15, 329–338. doi: 10.1016/j.chom.2014.02.009
- Luan, S., Lan, W., and Chul Lee, S. (2009). Potassium nutrition, sodium toxicity, and calcium signaling: connections through the CBL-CIPK network. *Curr. Opin. Plant Biol.* 12, 339–346. doi: 10.1016/j.pbi.2009.05.003
- Ma, W., and Berkowitz, G. A. (2011). Ca<sup>2+</sup> conduction by plant cyclic nucleotide gated channels and associated signaling components in pathogen defense signal transduction cascades. *New Phytol.* 190, 566–572. doi: 10.1111/j.1469-8137.2010.03577.x
- Macho, A. P., and Zipfel, C. (2014). Plant PRRs and the activation of innate immune signaling. *Mol. Cell.* 54, 263–272. doi: 10.1016/j.molcel.2014.03.028
- McAinch, M. R., and Pittman, J. K. (2009). Shaping the calcium signature. *New Phytol.* 181, 275–294. doi: 10.1111/j.1469-8137.2008.02682.x
- Mithofer, A., and Mazars, C. (2002). Aequorin-based measurements of intracellular Ca<sup>2+</sup>-signatures in plant cells. *Biol. Proced. Online* 4, 105–118. doi: 10.1251/bpo40
- Munns, R., and Tester, M. (2008). Mechanisms of salinity tolerance. *Annu. Rev. Plant Biol.* 59, 651–681. doi: 10.1146/annurev.arplant.59.032607.092911
- Nomura, H., Komori, T., Uemura, S., Kanda, Y., Shimotani, K., Nakai, K., et al. (2012). Chloroplast-mediated activation of plant immune signalling in *Arabidopsis*. *Nat. Commun.* 3, 926. doi: 10.1038/ncomms1926
- Pandey, G. K., Cheong, Y. H., Kim, K. N., Grant, J. J., Li, L., Hung, W., et al. (2004). The calcium sensor calcineurin B-like 9 modulates abscisic acid sensitivity and biosynthesis in *Arabidopsis*. *Plant Cell* 16, 1912–1924. doi: 10.1105/tpc.021311
- Ranf, S., Eschen-Lippold, L., Pecher, P., Lee, J., and Scheel, D. (2011). Interplay between calcium signalling and early signalling elements during defence responses to microbe- or damage-associated molecular patterns. *Plant J.* 68, 100–113. doi: 10.1111/j.1365-313X.2011.04671.x

- Ranf, S., Grimmer, J., Poschl, Y., Pecher, P., Chinchilla, D., Scheel, D., et al. (2012). Defense-related calcium signaling mutants uncovered via a quantitative high-throughput screen in *Arabidopsis thaliana*. *Molecular plant*, 5, 115–130. doi: 10.1093/mp/sss064
- Ranf, S., Wunnenberg, P., Lee, J., Becker, D., Dunkel, M., Hedrich, R., et al. (2008). Loss of the vacuolar cation channel, AtTPC1, does not impair Ca<sup>2+</sup> signals induced by abiotic and biotic stresses. *Plant J*, 53, 287–299. doi: 10.1111/j.1365-313X.2007.03342.x
- Rentel, M. C., and Knight, M. R. (2004). Oxidative stress-induced calcium signaling in *Arabidopsis*. *Plant Physiol*, 135, 1471–1479. doi: 10.1104/pp.104.042663
- Segonzac, C., and Zipfel, C. (2011). Activation of plant pattern-recognition receptors by bacteria. *Curr. Opin. Microbiol.*, 14, 54–61. doi: 10.1016/j.mib.2010.12.005
- Seybold, H., Trempel, F., Ranf, S., Scheel, D., Romeis, T., and Lee, J. (2014). Ca<sup>2+</sup> signalling in plant immune response: from pattern recognition receptors to Ca<sup>2+</sup> decoding mechanisms. *New Phytol.*, 204, 782–790. doi: 10.1111/nph.13031
- Shan, L., He, P., Li, J., Heese, A., Peck, S. C., Nurnberger, T., et al. (2008). Bacterial effectors target the common signaling partner BAK1 to disrupt multiple MAMP receptor-signaling complexes and impede plant immunity. *Cell Host Microbe*, 4, 17–27. doi: 10.1016/j.chom.2008.05.017
- Shimomura, O., Musicki, B., Kishi, Y., and Inouye, S. (1993). Light-emitting properties of recombinant semi-synthetic aequorins and recombinant fluorescein-conjugated aequorin for measuring cellular calcium. *Cell Calcium*, 14, 373–378. doi: 10.1016/0143-4160(93)90041-4
- Singh, R. P., Hodson, D. P., Huerta-Espino, J., Jin, Y., Bhavani, S., Njau, P., et al. (2011). The emergence of Ug99 races of the stem rust fungus is a threat to world wheat production. *Annu. Rev. Phytopathol.*, 49, 465–481. doi: 10.1146/annurev-phyto-072910-095423
- Smith, J. M., Salamango, D. J., Leslie, M. E., Collins, C. A., and Heese, A. (2014). Sensitivity to Flg22 is modulated by ligand-induced degradation and de novo synthesis of the endogenous flagellin-receptor FLAGELLIN-SENSING2. *Plant Physiol*, 164, 440–454. doi: 10.1104/pp.113.229179
- Spalding, E. P., and Harper, J. F. (2011). The ins and outs of cellular Ca(2+) transport. *Curr. Opin. Plant Biol*, 14, 715–720. doi: 10.1016/j.pbi.2011.08.001
- Stael, S., Wurzinger, B., Mair, A., Mehlmer, N., Vothknecht, U. C., and Teige, M. (2012). Plant organellar calcium signalling: an emerging field. *J. Exp. Bot.*, 63, 1525–1542. doi: 10.1093/jxb/err394
- Steinhorst, L., and Kudla, J. (2013). Calcium and reactive oxygen species rule the waves of signaling. *Plant Physiol*, 163, 471–485. doi: 10.1104/pp.113.222950
- Suzuki, N., Rivero, R. M., Shulaev, V., Blumwald, E., and Mittler, R. (2014). Abiotic and biotic stress combinations. *New Phytol.*, 203, 32–43. doi: 10.1111/nph.12797
- Swanson, S. J., Choi, W. G., Chanoca, A., and Gilroy, S. (2011). In vivo imaging of Ca<sup>2+</sup>, pH, and reactive oxygen species using fluorescent probes in plants. *Ann. Rev. Plant Biol.*, 62, 273–297. doi: 10.1146/annurev-arplant-042110-103832
- Tang, R. H., Han, S., Zheng, H., Cook, C. W., Choi, C. S., Woerner, T. E., et al. (2007). Coupling diurnal cytosolic Ca<sup>2+</sup> oscillations to the CAS-IP3 pathway in *Arabidopsis*. *Science*, 315, 1423–1426. doi: 10.1126/science.1134457
- Torres, M. A., Dangl, J. L., and Jones, J. D. (2002). *Arabidopsis* gp91phox homologues AtrbohD and AtrbohF are required for accumulation of reactive oxygen intermediates in the plant defense response. *Proc. Natl. Acad. Sci. U.S.A.*, 99, 517–522. doi: 10.1073/pnas.012452499
- Tracy, F. E., Gilliam, M., Dodd, A. N., Webb, A. A., and Tester, M. (2008). NaCl-induced changes in cytosolic free Ca<sup>2+</sup> in *Arabidopsis thaliana* are heterogeneous and modified by external ionic composition. *Plant Cell Environ.*, 31, 1063–1073. doi: 10.1111/j.1365-3040.2008.01817.x
- Traynelis, S. F., Wollmuth, L. P., McBain, C. J., Menniti, F. S., Vance, K. M., Ogden, K. K., et al. (2010). Glutamate receptor ion channels: structure, regulation, and function. *Pharmacol. Rev.*, 62, 405–496. doi: 10.1124/pr.109.002451
- Tsuda, K., and Katagiri, F. (2010). Comparing signaling mechanisms engaged in pattern-triggered and effector-triggered immunity. *Curr. Opin. Plant Biol.*, 13, 459–465. doi: 10.1016/j.pbi.2010.04.006
- Ward, J. M., Maser, P., and Schroeder, J. I. (2009). Plant ion channels: gene families, physiology, and functional genomics analyses. *Annu. Rev. Physiol.*, 71, 59–82. doi: 10.1146/annurev.physiol.010908.163204
- Yamada, K., Yamashita-Yamada, M., Hirase, T., Fujiwara, T., Tsuda, K., Hiruma, K., et al. (2016). Danger peptide receptor signaling in plants ensures basal immunity upon pathogen-induced depletion of BAK1. *EMBO J.*, 35, 46–61. doi: 10.15252/embj.201591807
- Yoshida, K., Schuenemann, V. J., Cano, L. M., Pais, M., Mishra, B., Sharma, R., et al. (2013). The rise and fall of the Phytophthora infestans lineage that triggered the Irish potato famine. *eLife*, 2, e00731. doi: 10.7554/eLife.00731
- Yuan, F., Yang, H., Xue, Y., Kong, D., Ye, R., Li, C., et al. (2014). OSCA1 mediates osmotic-stress-evoked Ca<sup>2+</sup> increases vital for osmosensing in *Arabidopsis*. *Nature*, 514, 367–371. doi: 10.1038/nature13593
- Zhang, J., Shao, F., Li, Y., Cui, H., Chen, L., Li, H., et al. (2007). A *Pseudomonas syringae* effector inactivates MAPKs to suppress PAMP-induced immunity in plants. *Cell Host Microbe*, 1, 175–185. doi: 10.1016/j.chom.2007.03.006
- Zhu, J. K. (2001). Plant salt tolerance. *Trends Plant Sci.*, 6, 66–71. doi: 10.1016/S1360-1385(00)01838-0
- Zhu, J. K. (2003). Regulation of ion homeostasis under salt stress. *Curr. Opin. Plant Biol.*, 6, 441–445. doi: 10.1016/S1369-5266(03)00085-2
- Zipfel, C. (2014). Plant pattern-recognition receptors. *Trends Immunol.*, 35, 345–351. doi: 10.1016/j.it.2014.05.004
- Zipfel, C., Kunze, G., Chinchilla, D., Caniard, A., Jones, J. D., Boller, T., et al. (2006). Perception of the bacterial PAMP EF-Tu by the receptor EFR restricts *Agrobacterium*-mediated transformation. *Cell*, 125, 749–760. doi: 10.1016/j.cell.2006.03.037

**Conflict of Interest Statement:** The authors declare that the research was conducted in the absence of any commercial or financial relationships that could be construed as a potential conflict of interest.

Copyright © 2017 Cao, Jiang, Yi, Yang, Ke, Pei and Zhu. This is an open-access article distributed under the terms of the Creative Commons Attribution License (CC BY). The use, distribution or reproduction in other forums is permitted, provided the original author(s) or licensor are credited and that the original publication in this journal is cited, in accordance with accepted academic practice. No use, distribution or reproduction is permitted which does not comply with these terms.